Original Research

MEDICAL IMAGING

Tumor size estimation of the breast cancer molecular subtypes using imaging techniques

Gulten Sezgın[1], Melda Apaydın[1], Demet Etıt[2], Murat Kemal Atahan[3]

1) Department of Radiology, Izmir Katip Celebi University Ataturk Training and Research Hospital, Turkey

2) Department of Pathology, Izmir Katip Celebi University Ataturk Training and Research Hospital, Turkey

3) Department of General Surgery, Izmir Katip Celebi University Ataturk Training and Research Hospital, Turkey

Abstract

Background and aim. In medical practice the classification of breast cancer is most commonly based on the molecular subtypes, in order to predict the disease prognosis, avoid over-treatment, and provide individualized cancer management. Tumor size is a major determiner of treatment planning, acting on the decision-making process, whether to perform breast surgery or administer neoadjuvant chemotherapy. Imaging methods play a key role in determining the tumor size in breast cancers at the time of the diagnosis.
We aimed to compare the radiologically determined tumor sizes with the corresponding pathologically determined tumor sizes of breast cancer at the time of the diagnosis, in correlation with the molecular subtypes.

Methods. Ninety-one patients with primary invasive breast cancer were evaluated. The main molecular subtypes were luminal A, luminal B, HER-2 positive, and triple-negative. The Bland-Altman plot was used for presenting the limits of agreement between the radiologically and the pathologically determined tumor sizes by the molecular subtypes.

Results. A significantly proportional underestimation was found for the luminal A subtype, especially for large tumors. The p-values for the magnetic resonance imaging, mammography, and ultrasonography were 0.020, 0.030, and <0.001, respectively. No statistically significant differences were observed among the radiologic modalities in determining the tumor size in the remaining molecular subtypes ($p>0.05$).

Conclusion. The radiologically determined tumor size was significantly smaller than the pathologically determined tumor size in the luminal A subtype of breast cancers when measured with all three imaging modalities. The differences were more prominent with ultrasonography and mammography. The underestimation rate increases as the tumor gets larger.

Keywords: breast cancer, molecular subtypes, tumor size, ultrasonography, mammography, magnetic resonance imaging

Introduction

Classification of breast cancer by molecular subtypes is commonly used in medical practice to predict the disease prognosis, avoid over-treatment, and provide individualized cancer management. The breast cancer molecular subtypes are mainly the luminal A, luminal B, human epidermal growth factor receptor 2 (HER2) positive, and triple-negative (TN) [1-4].

Imaging methods play a key role in the diagnosis of breast cancers. Mammography (MM), ultrasonography (US), and magnetic resonance imaging (MRI) are the commonly used methods to diagnose the diseases of the breast. Each of these imaging modalities has its advantages and disadvantages compared to each other in determining the tumor size [5].

Mammography can provide better images of suspected calcifications and tissue distortions compared to the other two

DOI: 10.15386/mpr-1476

Manuscript received: 23.09.2019
Received in revised form: 01.01.2020
Accepted: 20.01.2020

Address for correspondence:
sezgingulten@gmail.com

radiological modalities. However, the measurements are not free of limitations especially because of parenchymal superposition [6]. Although US allows tumor size measurements in multiple planes, it is operator dependent and associated with posterior acoustic shadowing, limiting the accurate the tumor size assessment. MRI allows multiplane imaging and provides more accurate results when the tumor is multifocal and multicentric, but false-positive findings and overestimations may also occur [7].

Tumor size is an important element of the clinical staging process that directly affects treatment planning and the patient's candidacy for oncoplastic breast surgery or neoadjuvant chemotherapy (NAC). To the best of our knowledge of the literature, there are only few studies investigating the relationship of the tumor size determination with the molecular subtypes of breast cancer at the time of the diagnosis. The previous studies in the literature have examined the response to neoadjuvant chemotherapy.

Our aim was to compare the imaging-determined tumor size with the pathologically confirmed tumor dimensions according to the molecular subtypes of breast cancer at the time of the diagnosis.

Material and methods

Patient selection

The study was approved by the local ethics committee. Because of the retrospective design of the study, the requirement for collecting informed consent from eligible patients was waived by our institutional review board. All breast imaging studies performed in our hospital in the period from January to June 2016 were screened retrospectively using the hospital local electronic archive of medical images. A total of 119 patients with primary breast cancer were included in this evaluation. MRI was performed in these patients besides US and MM in our institution due to the following indications which included multifocal and multicentric tumors, segmental/linear malignant calcifications, and dense breast parenchyma. We excluded patients with pure carcinoma in situ, patients who underwent NAC, patients with incomplete documentation, and patients with dense breast parenchyma in the MM as the latter could have affected the precise determination of the lesion size. Ninety-one patients were included in the study. All patients had preoperative MM, US and, MRI. The images were evaluated and reported only by one breast radiologist with nine years of experience.

The patients were evaluated by MM firstly. US examination and US-guided core biopsy procedures were performed on the same day. MRI examinations were performed within one week after MM and US imaging preoperatively. The radiologist was not blinded to the tumor size determined by the other imaging methods. The surgery operations were performed approximately one month after the imaging examinations. The pathological reports of the tumor sizes were obtained later and the radiologist was not informed of the pathologically determined tumor sizes.

Mammography

Mammograms were obtained with direct digital mammography (IMS Giotto, Italy). Standard MM was performed in craniocaudal and mediolateral oblique views. The largest tumor size was measured and included in the data analysis.

Ultrasonography

The US examination was performed with a high-frequency (13 MHz) linear transducer (Hitachi brand Ezu-MT 28- S1 model, Japan). Both breasts were screened in radial and anti-radial plans. The longest tumor axis was measured, excluding the hyperechoic rim around the tumor.

Magnetic resonance imaging

All examinations were performed with a 1.5 Tesla (T) MRI device (General Electric Signa HDx, GE Medical Systems, USA) using 8-channel phased-array breast surface coil. Care was taken to perform the breast MRI in the period between the 7th and 14th days of the menstrual cycle in pre-menopausal women. Conventional MRI images were obtained with the following techniques: axial fat-suppressed T2-weighted TR/TE 5500 msec/76 msec, field of view (FOV): 280 mm, matrix 384 × 384; number of excitations (NEX): 2; axial T1- weighted (TR/TE), 470 msec/11msec, FOV: 350 mm, NEX: 1, matrix 288 x 384; with slice thicknesses of 4 mm with a 1.2 mm intersection gap without contrast. The contrast agent (gadoterate meglumine Dotarem®, Guerbet; gadobutrol: Gadovist®, Bayer Healthcare) was administered at a dose of 0.1 mmol/kg using an automatic syringe (Medrad Spectris Solaris EP, Bayer Radiology Solutions) and this injection was followed by a 15–20 cc of saline flush. Six post-contrast dynamic sequences were taken at 60 seconds intervals with the following technical characteristics: TR/TE 5.02 msec/2.39 msec, FOV: 360 mm, matrix 253 x 352, NEX: 1, flip angle: 10°, 1.6 mm slice thickness, and a 1 mm intersection gap. Post-processing manipulation included the production of standard subtraction and maximum-intensity-projection images (MIP). The largest tumor size was measured on the MIP images.

Pathology

Pathologic assessments were performed by a dedicated breast pathologist. Tumor size was measured by gross and microscopic pathological examinations. The largest tumor size was taken into consideration in multifocal and/or multicentric tumors.

Histological types of tumors with molecular features were noted for each patient. Modified Bloom Richardson grading system was used for grading the tumors as grade 1, 2, and 3 [2]. Immunohistochemical staining was performed to examine estrogen receptors

(ER), progesterone receptors (PR), and the HER2 and Ki-67 antigens. The results were noted. Molecular subtypes were diagnosed according to their hormone receptor-positive and negative status as follows: Luminal A: ER+, PR+, HER2-, and low Ki-67 index; luminal B: ER+, PR+ or PR-, HER2- or HER2+, and high Ki-67 index; HER2+: ER-, PR-, HER2+, and finally TN: ER-, PR-, HER2- [2]. A Ki-67 index over 20% was accepted high by the pathology laboratory of our hospital.

Statistical analysis

Each size measurement of the tumor with each of the imaging modalities was compared with the corresponding tumor size determined by the pathological examination. The categorical variables were presented in frequencies and percentages. The numeric variables were presented in means and standard deviations. The Bland–Altman plot was used for presenting the limits of agreement between the radiologically and pathologically determined tumor sizes. The graph implied the degree to which the measured values fitted the normal expectation of agreement. For Bland–Altman plotting, the mean difference between the two measurements and a 1.96 standard deviation were calculated. The dotted lines showed the values with a ±1.96 confidence interval (CI). The difference between the two measurements was plotted against the average of the two measurements. The closer the average was to zero, the more accurate the measurement was. Linear regression was performed to detect any proportional bias in the Bland–Altman plotting. A p-value below 0.05 indicated a significantly proportional distortion below or above the average difference [8]. Similar to the study by Haraldsdottir, if the difference between the radiologically and pathologically determined tumor sizes was ≥10 mm, this was considered a clinically significant difference [9].

All analyses were conducted using statistical software (SPSS, version 17.0). A p-value of less than .05 was accepted statistically significant.

Results

The patients and tumor characteristics are shown in table I. The mean age was 53.8±13.4 years (median 51, range 31-90). The mean pathologically determined tumor size was 30.3±22.2 mm (median 25 mm, range 7-150 mm); the tumor size was determined to be 29.4±21.1 mm (median 24 mm, range 6-138 mm) with MRI, 20.1±8 mm (median 20 mm, range 5-141 mm) with MM, and 20.1±11.4 mm (median 18 mm, range 5-66 mm) with US. Thirty-two patients (35.2%) had multifocal or multicentric breast cancers. There were six cases of ductal carcinoma in situ (DCIS) accompanying the invasive tumor in our study. Four cases were subtyped as luminal A and two cases were subtyped as luminal B.

The 95% CI values showed the limits for all imaging modalities within the clinical significance threshold (<10 mm). The Bland–Altman plots were presented for luminal A in Figure 1. A significantly proportional underestimation was found for luminal A in the linear regression analysis. The p-values for MRI, MM, and US respectively were 0.020, 0.030, and < 0.001 in the luminal A subtype; they were 0.226, 0.050, and 0.410 in the luminal B subtype; they were 0.137, 0.290, and 0.094 in the HER2 + subtype, and they were 0.977, 0.978, and 0.257 in the TN subtype of breast cancers. All imaging modalities led to miscalculations in the tumor size in the luminal A breast cancers, especially in the large-size tumors (Figure 1). In the other subtypes, there were no statistically significant differences between the radiologically determined and pathologically determined tumor sizes.

Table I. Characteristics of breast cancer patients and molecular subtypes of tumors.

	Luminal A N=38	Luminal B N=32	HER2(+) N=6	TN N=15
Age (Mean, ± SD)	56.55±14.05	49.56±10.99	56.17±12.28	55.00±15.77
Diagnosis (n, %)				
Invasive ductal carcinomas	22 (57.9)	20 (62.5)	6 (100)	7 (46.7)
Invasive lobular carcinomas	8 (21.1)	6 (18.8)	0 (0)	0 (0)
Invasive ductolobular carcinomas	4 (10.5)	5 (15.6)	0 (0)	4 (26.7)
Other carcinomas	4 (10.5)	1 (3.1)	0 (0)	4 (26.7)
Grade (n, %)				
I	5 (13.2)	2 (6.3)	0 (0)	1 (6.7)
II	31 (81.6)	20 (62.5)	2 (33.3)	9 (60.0)
III	2 (5.3)	10 (31.3)	4 (66.7)	5 (33.3)
Pathological size, mm (mean= SD)	**30.7±22.2**	**29.6±14.5**	**24.2±10.3**	**33.2±36.4**
MRI size, mm (mean= SD)	**26.9±17.7**	**29.4±16.5**	**25.5±7.4**	**37.5±36.5**
MM size, mm (mean= SD)	**22.3**±14.9	23.1±12.0	21.3±8.5	35.9±39.4
US size, mm (mean= SD)	17.4±9.7	26.3±12.8	20.4±7.1	20.0±10.9

HER2 (+): Human epidermal growth factor 2 positive breast cancer; TN: Triple negative breast cancer; MRI: Magnetic resonance imaging; MM: Mammography; US: Ultrasonography; SD: Standard deviation

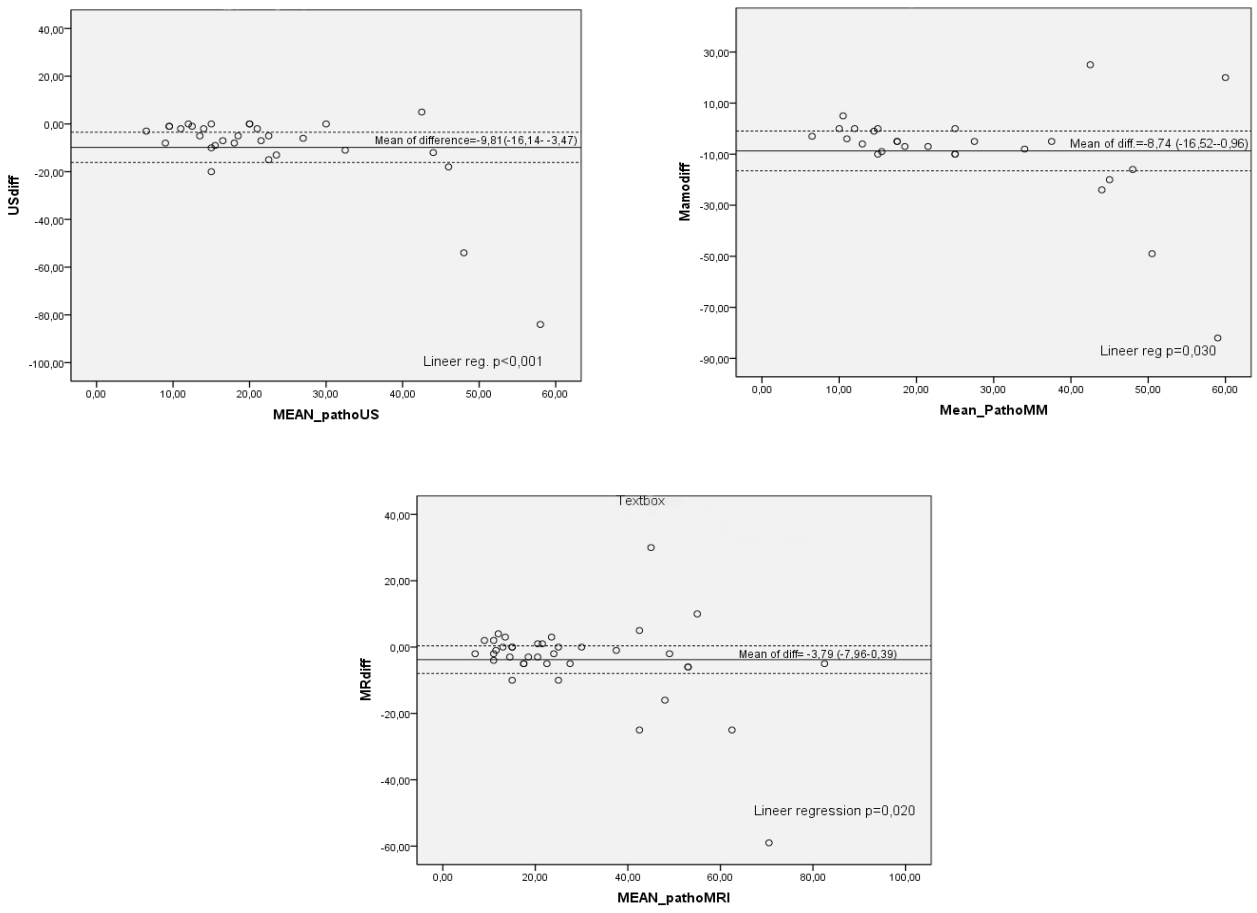

Figure 1. Bland Altman plot shows the size difference between US, MM and, MRI with pathological size for luminal A breast cancer. MRI diff: Magnetic resonance imaging size difference; MM diff: Mammography size difference; US diff: Ultrasonography size difference; patho: pathologic size.

Table II. The deviation values of radiological size from pathological size in molecular subtypes according to Bland Altman graphs (Bland-Altman graphs are not shown except for luminal A subtype).

Tumor subtypes	For US (mod, mm)	For MM (mod, mm)	For MRI (mod, mm)
Luminal A	-9.81	-8.74	-3.79
Luminal B	-5.46	-6.48	0.19
HER 2+	-2.60	-1.25	1.33
TN	-0.67	3.55	4.27

Table III. The over-underestimation ratios of imaging modalities according to molecular subtype breast cancers.

		MRI n (%)	MM n (%)	US n (%)
Luminal A	Overestimation	2 (2.19)	3 (3.29)	3 (3.29)
	Underestimation	5 (5.49)	10 (10.98)	9 (9.89)
Luminal B	Overestimation	6 (6.59)	2 (2.19)	3 (3.29)
	Underestimation	5 (5.49)	8 (8.79)	7 (7.69)
HER 2+	Overestimation	- (0)	- (0)	- (0)
	Underestimation	-(0)	1 (1.09)	1 (1.09)
TN	Overestimation	4 (4.39)	2 (2.19)	1 (1.09)
	Underestimation	- (0)	- (0)	- (0)
Total	Overestimation	12 (13.18)	7 (7.69)	7 (7.69)
	Underestimation	10 (10.98)	19 (20.87)	17 (18.68)

MRI: magnetic resonance imaging, MM: mammography, US: ultrasonography, HER 2+: human epidermal growth factor receptor 2 positive breast cancer, TN: triple negative breast cancer

According to the Bland Altman graphs, the differences between the radiologically and pathologically determined sizes are presented by the molecular subtypes in Table II. MRI was the modality, which provided the most precise measurements within the narrowest CI in the luminal A subtype of breast cancer.

In comparison, the imaging modalities inaccurately measured the tumor size in 22 (24.18%) cases on MRI; 26 (28.57%) cases on MM and 24 (26.37%) cases on US. The over-underestimation rates according to molecular subtypes are given in detail in Table III.

A moderate or marked level of background parenchymal enhancement (BPE) was observed in 19 patients (20.88%).

Discussion

This study has shown that the radiologically determined tumor size in the luminal A subtype of breast cancer is significantly smaller than the pathologically determined tumor size in all of the three imaging modalities. The underestimation rate increases as the tumor gets larger.

It is known that the luminal-A subtype has a better prognosis; however, it is associated with a poor chemotherapy response [10]. Chemotherapy has been reported to be controversial for lymph node-positive patients with the luminal-A subtype breast cancer [10]. Thus, surgery and achieving negative surgical margins are critical.

Luminal A and B cancers approximately account for 70% of the breast cancers with positive hormone receptors [1]. In our study, compatible with the overall distribution, the rates of the luminal A (41.8%) and luminal B (35.2%) subtypes reached a total rate of 77%.

Luminal A and B cancers are usually examined in one category to report imaging findings; which are characterized by the image of a mass with poorly circumscribed margins and posterior acoustic shadowing (Figure 1). A high Ki-67 level is an indicator of poor prognosis and it is used as a parameter to classify the luminal cancers [2]. We assigned the luminal cancers with Ki-67 levels >20 into the group of luminal B subtype. The underestimation rates of luminal A cancers were found out to be different from those in the luminal B group in our study (Table III). All invasive lobular carcinomas in our case series were of the luminal subtypes (Table I). Furthermore, the most prominently underestimated cases were the invasive lobular carcinoma cases. It is accepted that invasive lobular carcinoma can easily be underestimated with the following radiological techniques; MM, MRI, and US [5,11,12].

We detected that the tumor grades were significantly different between the luminal A and B tumors. Lacroix et al. have reported that grade 1 and grade 2 tumors show stromal reactions with spicules and perilesional hyperechoic halos, while grade 3 tumors do not develop stromal reactions and they are round-shaped in the US examinations [13]. In the literature, it is reported that perilesional hyperechoic halos are more common in the luminal A subtype. Some studies have suggested that the underestimation can be reduced by including the surrounding halo to the area of measurement in the invasive tumors [14,15]. We did not measure the hyperechoic halo around the tumor. This may be a reason for our underestimations in luminal A cases.

It has been reported that luminal breast cancer is highly associated with DCIS [1,16]. Hieken et al. have reported that the underestimation in the sonographic examination occurs because of the in situ component of the tumor with indefinite edge features [14]. Also, it has been reported that it is difficult to determine the precise dimensions of the tumor with radiological methods in DCIS [17]. However; in our study, the underestimation rates were not associated with the presence of DCIS because the patients with accompanying DCIS diagnosis constituted a very small group.

We found out that the tumor size was larger (30.7±22.2 mm) in the luminal A breast cancers compared to the luminal B and HER 2+ breast cancers (Table 1). In our study, as in Gruber's, the underestimation increased as the tumor size reached 4 cm or larger [5]. Bosch et al. have reported that this might be related to the size of the transducer and suggested that the panoramic US should be used for visualizing the image of the lesion completely [4]. However, that method was not used in our study patients. A part of our underestimation may be related to this.

In the MM examinations, the tumor size measurements were significantly underestimated in the luminal A cancers (Figure 1). Heiken et al. have shown that the tumor size is measured smaller than the real tumor size because of high compression applied during MM [14]. Dense breast parenchyma is one of the leading causes that can impair measuring the tumor size precisely with MM [5]. However, the dense breast parenchyma was not a factor for the underestimation of the tumor size in our study, because mammograms were excluded, in which the tumor size cannot be measured.

Park et al. have compared the accuracies of MM, digital breast tomosynthesis (DBT), automated breast ultrasound, and MRI in evaluating the residual tumor size were compared in breast cancers after NAC [18]. In this study it was reported that MRI and DBT allowed assessing the tumor size more accurately in alignment with the pathological sizes. Our aim was to compare the radiologically and pathologically determined tumor sizes by the molecular subtypes at the time diagnosis, which was a different study aim from that of Park et al.'s study [18].

Although some studies have used MRI as the only diagnostic method and suggested a threshold value of 5 mm [19,20]. Unlike those studies, we used three different diagnostic methods (US, MM, and MRI) for measuring the tumor size and we excluded the patients with pure DCIS and we selected the threshold value of 10 mm in line with the study of Haraldsdottir [9].

Our incorrect estimation rates with MRI were similar to those reported in Yoo's study [19]. Our overestimation and underestimation rates were 13.18% and 10.98%, respectively; while Yoo et al. have reported the respective rates of 11.7% and 13.7%.

Background parenchymal enhancement is a normal breast tissue enhancement on MRI [21]. Leddy has reported that moderate and marked BPE, which is difficult to differentiate from non-mass enhancement, is a cause of incorrect determinations and it is a diagnostic limitation of MRI [7]. In our study, 20.88% (19/91) of the patients have moderate or marked levels of BPE while this rate was 32% in Leddy's study. There were only 7 cases with incorrect measurements among our cases. We think that BPE did not play a role in our rates of incorrect measurements because of the limited number of patients with moderate and marked BPE.

In our study, the numbers of HER 2+ (6.6%) and TN cancers (16.5%) were low. HER2+ tumors and TN tumors comprise 15% - 25% and 10% - 20% of all breast cancers, respectively [1]. HER 2+ cancers are characterized by irregular contours, dense parenchyma, pleomorphic microcalcifications, and multicentric and/or multifocal disease [5,22]. Triple-negative cancers have the most definitive imaging findings among the other molecular subtypes. Their findings are similar to benign masses on MM and US. These lesions have well-defined and smooth contours, demonstrate unifocal mass formation, and accompanied by posterior acoustic enhancement on US. Additionally, they show T2 hyperintense foci internally and rim enhancement on MRI. It is argued that the in situ carcinoma stage has been neglected due to the rapid progression in TN cancers [23,24]. In our study, among the three radiological modalities of tumor size measurements, the least deviations in the measured tumor size were observed on US in TN cancers. Deviations were very low in HER 2+ cases, in all modalities. However, because of the low number of cases in these two groups, results should be interpreted with caution.

There were several limitations in our study. Firstly, this is a retrospective and a single-center study. Secondly, the study sample is small because we included only the patients with MRI, US, and MM images, which allowed tumor size measurements. Thirdly, there is only one breast radiologist staff in our institution, not allowing us to perform an interobserver agreement assessment in this study.

Conclusion

We have shown in this study that the radiologically measured tumor size is significantly smaller than the pathologically measured tumor size in luminal A breast cancers. The likelihood of underestimation increases as the tumor gets larger. The discordance between the radiological and pathological measurements in the luminal A subtypes should be kept in mind in the decision-making process to select the appropriate treatment options, which would be oncoplastic surgery planning or NAC. Also, we have shown that there were no significant discrepancies between the radiological and pathological measurements of the tumor sizes in the luminal B, HER2 +, and TN breast cancers. Further prospective and multicenter studies are needed to support these results.

Acknowledgment

The statistical analyzes of this study was performed by Işıl ERGIN.

References

1. Cho N. Molecular subtypes and imaging phenotypes of breast cancer. Ultrasonography. 2016;35: 281-288.
2. Çelebi F, Pilancı KN, Ordu Ç, Ağacayak F, Alço G, İlgün S, et al. The role of ultrasonographic findings to predict molecular subtype, histologic grade, and hormone receptor status of breast cancer. Diagn Interv Radiol. 2015;21:448-453.
3. Simpson PT, Reis-Filho JS, Gale T, Lakhani SR. Molecular evolution of breast cancer. J Pathol. 2005;205:248-254.
4. Bosch AM, Kessels AG, Beets GL, Rupa JD, Koster D, van Engelshoven JM, et al. Preoperative estimation of the pathological breast tumour size by physical examination, mammography and ultrasound: a prospective study on 105 invasive tumours. Eur J Radiol. 2003;48:285-292.
5. Gruber IV, Rueckert M, Kagan KO, Staebler A, Siegmann KC, Hartkopf A, et al. Measurement of tumour size with mammography, sonography and magnetic resonance imaging as compared to histological tumour size in primary breast cancer. BMC Cancer. 2013;13:328.
6. Feig SA. Breast masses. Mammographic and sonographic evaluation. Radiol Clin North Am. 1992;30:67-92.
7. Leddy R, Irshad A, Metcalfe A, Mabalam P, Abid A, Ackerman S, et al. Comparative accuracy of preoperative tumor size assessment on mammography, sonography, and MRI: Is the accuracy affected by breast density or cancer subtype? J Clin Ultrasound. 2016;44:17-25.
8. Giavarina D. Understanding Bland Altman analysis. Biochem Med (Zagreb). 2015;25:141-151.
9. Haraldsdóttir KH, Jónsson Þ, Halldórsdóttir AB, Tranberg KG, Ásgeirsson KS. Tumor Size of Invasive Breast Cancer on Magnetic Resonance Imaging and Conventional Imaging Mammogram/Ultrasound): Comparison with Pathological Size and Clinical Implications. Scand J Surg. 2017;106:68-73.
10. Sun Y, Liu X, Cui S, Li L, Tian P, Liu S, et al. The inconsistency of molecular subtypes between primary foci and metastatic axillary lymph nodes in Luminal A breast cancer patients among Chinese women, an indication for chemotherapy? Tumour Biol. 2016;37:9555-9563.
11. Vijayaraghavan GR, Vedantham S, Santos-Nunez G, Hultman R. Unifocal Invasive Lobular Carcinoma: Tumor Size Concordance Between Preoperative Ultrasound Imaging and Postoperative Pathology. Clin Breast Cancer. 2018;18:e1367-e1372.
12. Berg WA, Gutierrez L, NessAiver MS, Carter WB, Bhargavan M, Lewis RS, et al. Diagnostic accuracy of mammography,

clinical examination, US, and MR imaging in preoperative assessment of breast cancer. Radiology. 2004;233:830-849.

13. Boisserie-Lacroix M, Mac Grogan G, Debled M, Ferron S, Asad-Syed M, Brouste V, et al. Radiological features of triple-negative breast cancers (73 cases). Diagn Interv Imaging. 2012;93:183-190.
14. Hieken TJ, Harrison J, Herreros J, Velasco JM. Correlating sonography, mammography, and pathology in the assessment of breast cancer size. Am J Surg. 2001;182:351-354.
15. Meier-Meitinger M, Häberle L, Fasching PA, Bani MR, Heusinger K, Wachter D, et al. Assessment of breast cancer tumour size using six different methods. Eur Radiol. 2011;21:1180-1187.
16. Jansen SA. Ductal carcinoma in situ: detection, diagnosis, and characterization with magnetic resonance imaging. Semin Ultrasound CT MR. 2011;32:306-318.
17. Newstead GM. MR imaging of ductal carcinoma in situ. Magn Reson Imaging Clin N Am. 2010;18:225-240.
18. Park J, Chae EY, Cha JH, Shin HJ, Choi WJ, Choi YW, et al. Comparison of mammography, digital breast tomosynthesis, automated breast ultrasound, magnetic resonance imaging in evaluation of residual tumor after neoadjuvant chemotherapy. Eur J Radiol. 2018;108:261-268.
19. Yoo EY, Nam SY, Choi HY, Hong MJ. Agreement between MRI and pathologic analyses for determination of tumor size and correlation with immunohistochemical factors of invasive breast carcinoma. Acta Radiol. 2018;59:50-57.
20. Choi WJ, Cha JH, Kim HH, Shin HJ, Chae EY. The Accuracy of Breast MR Imaging for Measuring the Size of a Breast Cancer: Analysis of the Histopathologic Factors. Clin Breast Cancer. 2016;16:e145-e152.
21. You C, Kaiser AK, Baltzer P, Krammer J, Gu Y, Peng W, et al. The Assessment of Background Parenchymal Enhancement (BPE) in a High-Risk Population: What Causes BPE? Transl Oncol. 2018;11:243-249.
22. Grimm LJ, Johnson KS, Marcom PK, Baker JA, Soo MS. Can breast cancer molecular subtype help to select patients for preoperative MR imaging? Radiology. 2015;274:352-358.
23. Dogan BE, Turnbull LW. Imaging of triple-negative breast cancer. Ann Oncol. 2012;23 Suppl 6:vi23-vi29.
24. Uematsu T, Kasami M, Yuen S. Triple-negative breast cancer: correlation between MR imaging and pathologic findings. Radiology. 2009;250:638-647.